



## AAID Foundation Research Grant Report

**Grant Report Instructions:** The report should not be ten pages long. The page limit does not include the draft JOI manuscript.

**Principal Investigators:** W. Benton Swanson

**Co-Investigator:** Yuji Mishina

**Project title:** *Mineralized Synthetic Polymer Scaffold for Cell-free Osseous Wound Healing & Periodontal Tissue Engineering*

**Grant Period:** 09/01/2020 – 08/31/2023

**Objectives:** Healthy bone is critically essential to systemic health. Of relevance to the craniofacial complex, dental implants require that empty sockets be filled with bone before implant placement and dentition are restored. Bone quality and bone amount are strongly correlated with both dental implants' short- and long-term success. Biomaterials-based bone regeneration is promising to circumvent shortcomings of bone grafting. Recently, progress in guided bone regeneration demonstrates the role of both physical and chemical cues in biomaterial scaffolds to guide bone regeneration. Collagen-based matrices have been used in clinical periodontology for over two decades as space-filling matrices in mandibular and maxillary defects to prepare adequate bone for stable implant placement. Synthetic biomaterials that mimic the advantageous properties of collagen are desirable for their tunable properties, large-scale manufacturing potential, batch-to-batch consistency, and chemical functionality. Poly-spirolactams, notably polylactic acid (PLA), are among the most widely used synthetic biomaterials approved by the US Food and Drug Administration for biocompatibility and predictable biodegradation. However, due to their chemical structure, these materials commonly used to fabricate tissue engineering scaffolds need more inherent chemical functionality to increase biological specificity and functionality-inducing tissue fate. We have developed a synthetic strategy to impart favorable properties to PLA scaffolds, including their clinical handling properties. It is essential to maintain the horizontal and vertical dimensions of a bony defect at an implant or ridge site and induce its mineralization through nucleation sites chemically engineered into the material. *The overall therapeutic goal of this project is to exploit the regenerative capacity of endogenous mesenchymal stem cells by mimicking the extracellular matrix of resorbed bone with a polymeric tissue engineering construct through novel synthetic strategies.*

**Project Results:**

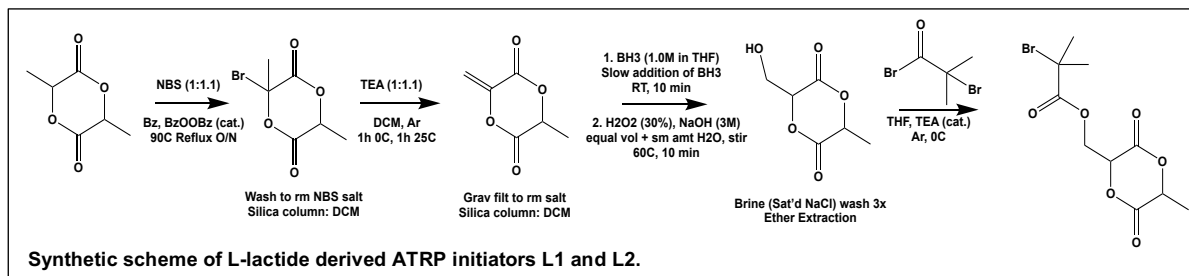


Mature mineralized bone tissue is defined by its vascularization and extracellular matrix (ECM) composition, two critical tissue-level properties. Type I collagen accounts for approximately 90% of matrix protein content in bone. The resulting collagen I matrix is mineralized by excreting membrane-bound matrix vesicles containing concentrated calcium and phosphate ions. This nanofibrous matrix is shown to be highly advantageous for tissue regeneration. Therefore, the ideal synthetic GBR construct should mimic this texture. Scanning electron micrograph (SEM) images of resorbed bone demonstrate a fibrillar, roughened surface texture resulting from the exposed collagen ECM, which is hypothesized to be a critical biophysical cue for bone regeneration. A thermally-induced phase separation technique is used to fabricate highly porous

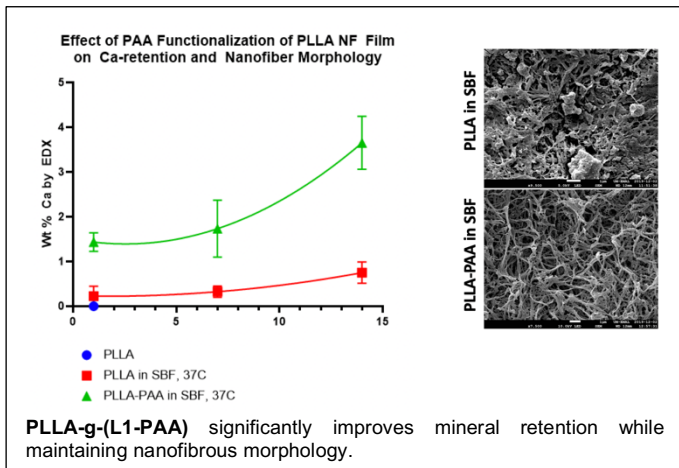
nanofibrous (NF) materials from poly (L-lactide) (PLLA), with fibers that mimic the triple-stranded helical structure of collagen, the primary component of the natural ECM (50 to 500 nm fiber diameter).

## 1) Engineering sites for mineralization

The high surface area of NF macroporous scaffolds is ripe for chemical functionality, imparted by incorporating oligomers synthesized by atom transfer radical polymerization (ATRP). ATRP is a living polymerization method allowing exceptionally well-controlled and uniform polymer molecular weights following a linear growth trajectory. We optimized the synthesis for two ATRP initiator molecules based on L-lactide, which was not previously reported (L1 and L2). These serve as chain ends for the polymerization of poly(acrylic acid) (PAA) from the terminal bromine of L1 and L2 (LX). Initially, we had proposed the use of poly(tertiary butyl acrylate) (PtBA), which was later hydrolyzed to poly(acrylic acid) (PAA), which was synthetically challenging. PAA is capable of binding calcium minerals *in situ*. Our kinetics data supports linear first-order growth kinetics, characteristic of ATRP polymerizations, with a UV-initiated metal-free ATRP system.



Nanofiber formation by thermally induced phase separation relies on high molecular weight crystalline poly (L-lactic acid) PLLA. To form a nanofibrous PLLA matrix, L1-PAA is copolymerized with L-lactide monomer via ring-opening polymerization, catalyzed by  $\text{Sn}(\text{Oct})_2$  catalyst. Nuclear magnetic resonance spectroscopy (NMR) confirms synthesis for molecular identity and purity. Given that L1 was synthesized in a much higher yield, we chose to use L1-PAA as our monomer of choice with the notion that it is synthetically more favorable for scaling up in a commercial process.



L1-PAA was assayed for its calcium-binding capacity, compared to commercially available PLLA, in simulated body fluid (SBF) by a colorimetric method (1,2-bis(o-aminophenoxy)ethane-N,N,N', N'-tetraacetic acid, BAPTA assay). Surface topographic analysis by SEM demonstrated the presence of uniform nanofibers; following incubation in SBF, PLLA-g-(L1-PAA) nanofibers retained more calcium than PLLA alone while maintaining the nanofibrous morphology after two weeks. One important consideration is whether the nucleation process precludes the porosity of our material. We did not investigate this aspect but hypothesize that a controlled

incubation over a short time may not be problematic.

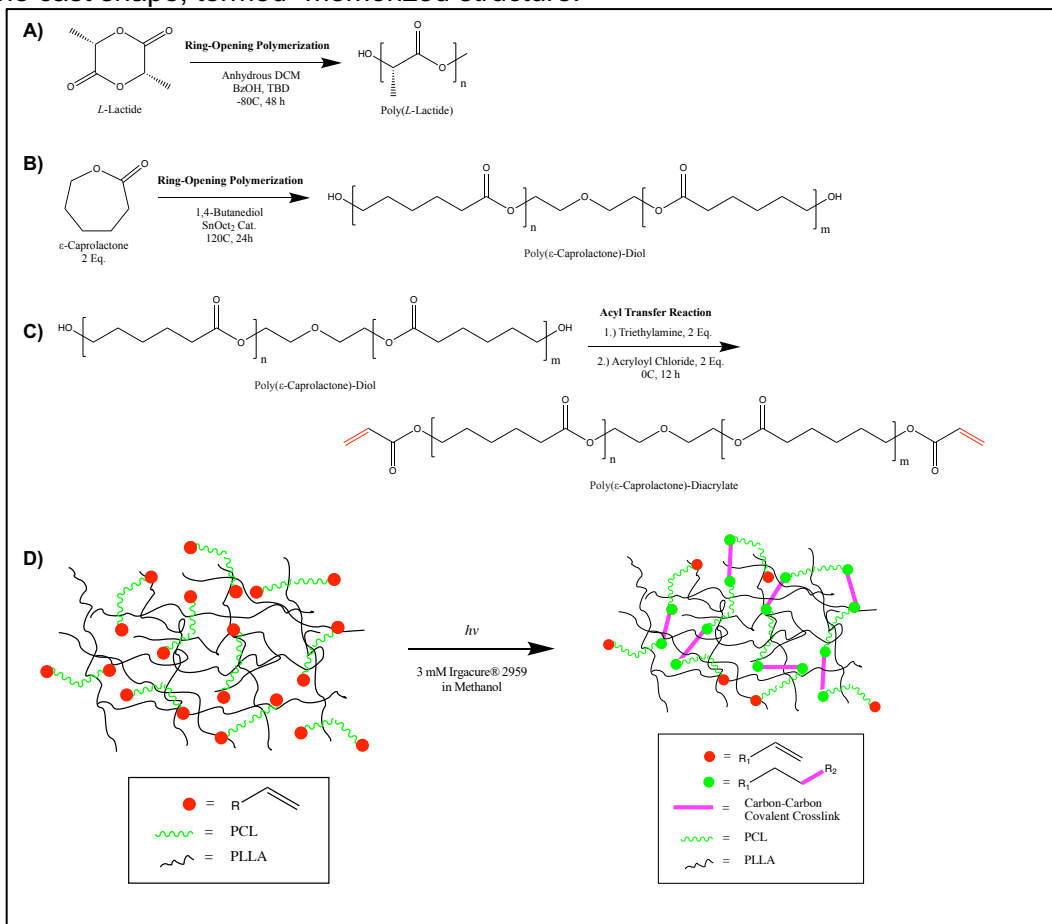
## 2) Engineering shape maintenance properties of a synthetic biomaterial

While we demonstrated an ability to synthesize synthetic nanofibers with nucleation sites for calcium mineral deposition, a persistent challenge in implementing this type of technology is its clinical handling. In the case of periodontal membranes, one of the significant challenges with current membrane technologies is their limited mechanical handling properties, particularly in maintaining the horizontal and vertical dimensions of the periodontal defect. This limitation is crucial in defects where space maintenance is essential for adequate bone regeneration to support a future prosthesis or dental implant. To address this, clinicians have employed titanium tenting screws and titanium-reinforced membranes to provide structural support to the membrane and prevent collapse into the defect. Titanium tenting screws can lead to increased clinical complexity and potential complications such as screw loosening or exposure and subsequent risk of infection. While providing rigidity, titanium-reinforced membranes can be difficult to adapt to the defect's contours and may lead to soft tissue complications if exposed. In the case of scaffolds or 3D space-filling matrices, a significant shortcoming in their clinical adoption is the need for handling properties that allow for their deformation without irreversibly disrupting their favorable morphology, which we and others have previously elucidated. In addition, biomaterial scaffolds must come into contact with the bone; ill-fitting interfaces between tissue engineering matrices or grafts and the defect margin lead to poor healing outcomes due to fibrous tissue formation, inflammatory infiltrate, increased risk of infection, and resorption. Therefore, a biomaterial capable of conformal fitting and volumetric filling of its highly porous internal structure is highly desirable. In the context of bone augmentation, the next generation of biomaterials must account for key processes involved in bone formation and enable therapeutic properties of the biomaterial construct to improve the predictability of outcomes. Both intramembranous and endochondral ossification processes heavily rely on the ingrowth of vasculature to supply nutrients, oxygen, and essential signaling factors. Therefore, it becomes crucial for biomaterial scaffolds to possess patent pores in situ that facilitate the infiltration and proliferation of endothelial and mesenchymal cells, ensuring adequate angiogenesis and subsequent bone development.

We developed a novel thermosensitive memorized microstructure (TS-MMS) tissue engineering scaffold, taking advantage of the favorable properties of PLLA and PCL to create a synthetic materials platform that allowed for deformation and recovery of the internal structures.

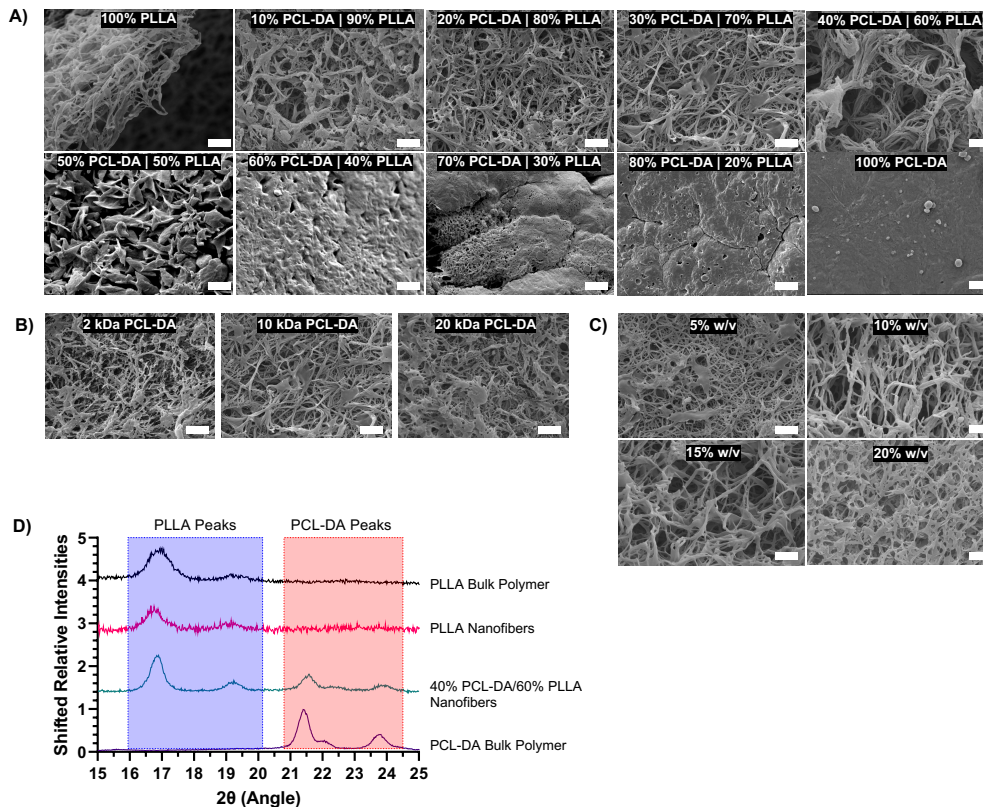
We use low molecular weight PCL-DA, a photopolymerizable PCL oligomer, to fabricate interpenetrating copolymer meshes in various PCL-DA/PLLA compositions to determine the boundary conditions for nanofiber formation and thermoresponsive properties. We demonstrate the reversible deformation of TS-MMS scaffolds above a critical temperature of 52°C. We assess their ability to facilitate cell and tissue infiltration *in vivo* after deformation and recovery, demonstrating their advantageous memorized microstructure recovery. This feature allowed us to modify the shape of the scaffolds at 52°C to achieve conformal fitting to the abnormally shaped defects, regaining their original mechanical rigidity upon cooling to physiologic temperature. Acellular TS-MMS scaffolds implanted subcutaneously enable robust vascularization and extracellular matrix deposition, demonstrating a proof of concept for their ability to facilitate robust tissue integration. These materials are critical for off-the-shelf synthetic, biodegradable materials fabricated at scale with favorable clinical handling properties.

We hypothesized that a thermosensitive biomaterial with memorized microstructure might be fabricated by the *in-situ* polymerization of a thermosensitive polyester mesh, PCL, within a rigid, high molecular weight PLLA matrix. PLLA and PCL are synthesized by ring-opening metastasis polymerization. The terminal functional groups of PCL are acrylate-modified by nucleophilic substitution with acryloyl chloride. Low molecular weight PCL-DA oligomers (2-20kDa) are dissolved in solution with high molecular weight PLLA (150 kDa), cast to a specified shape, and subjected to photoinitiated radical polymerization causing the chain extension PCL-DA in the cast shape, termed “memorized structure.”



To determine the ability of this semi-interpenetrating polymer mesh to form nanofibers, we synthesized two-dimensional thin films with varying compositions and evaluated nanofiber

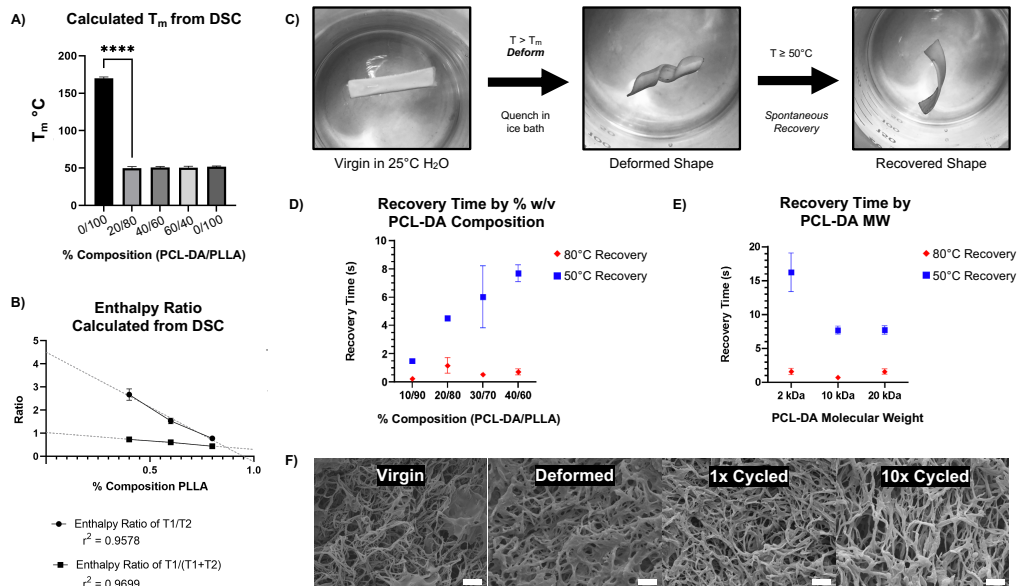
formation by scanning electron microscopy. Nanofibers formed at 0% w/w PCL-DA up to 40% w/w PCL-DA, where the remaining composition is PLLA, are indistinguishable. A platelet morphology is observed at 50% PCL-DA/50% PLLA. Beyond 60% PCL-DA incorporation, nanofiber morphology is lost due to the amorphous structure of PCL-DA. At 40% PCL-DA/60% PLLA, the molecular weight of PCL-DA does not affect nanofiber formation when PLLA molecular weight is held constant. Similarly, nanofibers are formed at 40% PCL-DA 10kDa/60% PLLA up to 20% total material w/v when cast from solution. Small angle x-ray scattering demonstrates the maintenance of PLLA crystallinity with characteristic peaks<sup>24</sup> at  $2\theta = 17^\circ, 19^\circ$ , preserved when fabricated as nanofibers and combined with PCL-DA at up to 40% PCL-DA/60% PLLA.



Dynamic scanning calorimetry demonstrates a marked reduction in T1 melting temperature ( $T_m$ ) from  $165^\circ\text{C}$  to  $52^\circ\text{C}$  upon incorporating PCL-DA. It remains the same irrespective of the relative composition of PCL-DA, which is comparable to PCL-DA alone. Where T1 is  $52^\circ\text{C}$ , corresponding to the melting temperature of PCL-DA, a T2 exists at  $165^\circ\text{C}$ , corresponding to the PLLA component (data not shown). Incorporating PCL-DA introduces a partial melting temperature to the PLLA matrix at a significantly lower temperature (T1). The enthalpy ratio of PCL-DA to PLLA (T1/T2) and PCL-DA to the total material (T1/(T1+T2)) is inversely proportional to the relative PLLA contribution to the entire material composition, enabling stoichiometric titration of temperature-sensitivity.

We hypothesized that materials were readily deformable at temperatures above  $T_m$  and recoverable to their original 3D morphology at the macro, micro, and nano scales. We developed an assay to determine shape recovery, where virgin materials were subjected to a warm water bath at  $T > T_m$  for 1 minute, then deformed and quenched in an ice bath to prevent recovery. Quenched materials are reintroduced to warm water baths at either  $80^\circ\text{C}$  or  $50^\circ\text{C}$ , and their spontaneous recovery is recorded using a digital camera for quantitative video frame analysis. At

80°C and 50°C, 100% PLLA materials are neither deformable without yielding nor recoverable, as expected. At 80°C ( $T > T_m$ ), all TS-MMS compositions, as low as 10% PCL-DA, exhibit rapid recovery; at 50°C ( $T \approx T_m$ ), the recovery time is directly proportional to the relative composition by PCL-DA within the range of compositions capable of forming biomimetic nanofibers. At 40% PCL-DA/60% PLLA, scaffolds with 2kDa PCL-DA recovered more slowly than 10kDa and 20 kDa at 50°C; no difference was observed at 80°C where all formulations recovered rapidly. After deformation and recovery, TS-MMS nanofibers are indistinguishable from virgin material. Even after ten cycles of deformation and recovery, nanofibers remain indistinguishable. For all subsequent fabrication, 40% PCL-DA (10 kDa)/60% PLLA was used to maximize thermosensitive shape recovery in subsequent validation experiments.



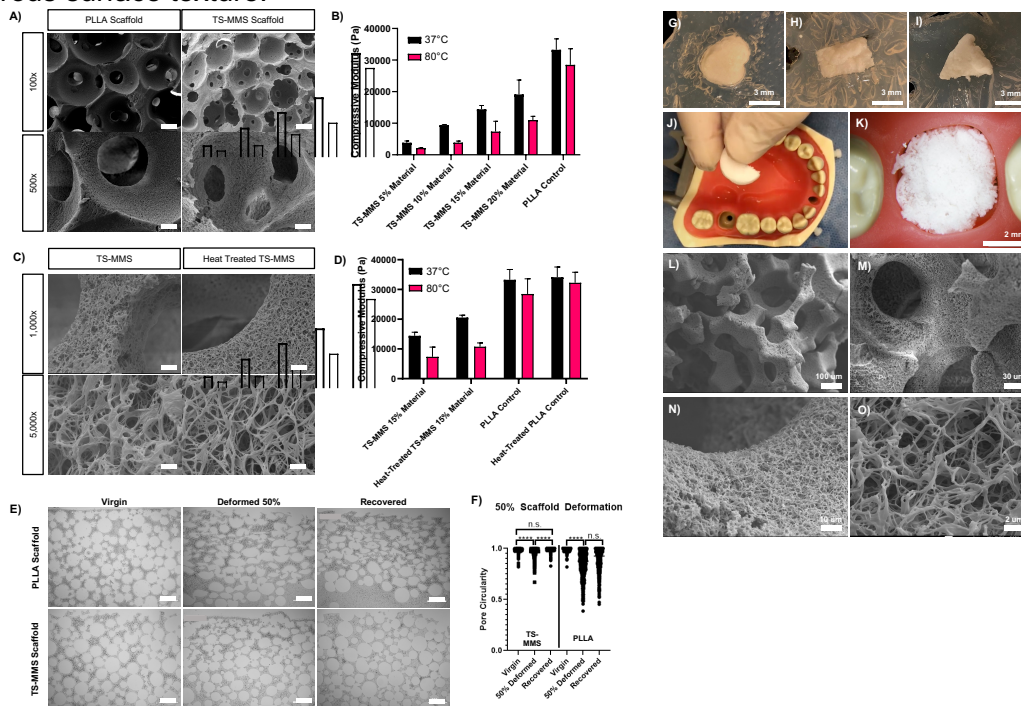
Nanofibrous, macroporous scaffolds were fabricated by a sugar sphere porogen method in situ polymerization of the TS-MMS and thermally induced phase separation, yielding scaffolds indistinguishable from PLLA control scaffolds by SEM. The compressive modulus of TS-MMS scaffolds varies as a function of total material weight percent as fabricated and is less than PLLA at the same composition (15% w/v). The compressive moduli of TS-MMS scaffolds, but not PLLA, decrease significantly at  $T > T_m$  (80°C). We hypothesized that heat treatment of the TS-MMS scaffolds would improve their mechanical properties by annealing PCL-DA within the confines of the crosslinked matrix to adopt minimum energy organization at a temperature between  $T_1$  and  $T_2$ , such that PLLA does not melt. TS-MMS scaffolds were heat treated at 75°C for 60 minutes, then cooled to room temperature. SEM micrographs show no adverse effect of heat treatment on nanofiber formation and a marked increase in compressive modulus of the 15% w/v TS-MMS scaffold at 37°C. No significant change was noted in the mechanical properties of virgin versus heat-treated PLLA scaffolds, attributing the transformation to the PCL component.

We hypothesized that TS-MMS fabrication and in situ polymerization of PCL-DA within the sugar sphere template would enable memorization of spherical macropore architecture and their recovery. 15 mm round TS-MMS and PLLA scaffolds were heated at 55°C for 5 minutes, then deformed by compressing in a mechanical tester to 50% of their height (3.0 mm, compressed by 1.5 mm) and quenched at 0°C in the deformed state. Then, scaffolds were placed in a 55°C water bath to recover for 5 minutes and cooled to room temperature. Virgin, deformed, and recovered

scaffolds from PLLA and TS-MMS were subjected to bulk serial sectioning and histologic analysis for macropore circularity. Image analysis of 40% PCL-DA/60% PLLA scaffolds demonstrates significant pore deformation, and recovery is insignificantly different from that of the virgin scaffold.

On the other hand, 100% PLLA scaffolds are deformed and fail to recover, with deformed and recovered pore circularity not significantly different. Notably, there was no significant difference between the macropore circularity of the virgin and recovered TS-MMS scaffold, suggesting that the macropores were not damaged during the thermosensitive cycle.

As proof of principle, circular TS-MMS scaffolds were deformed to fit irregular shapes cut from agar. We demonstrated using a semi-circle TS-MMS scaffold to fit a tooth extraction socket defect in a plastic typodont. SEM micrographs show maintenance of the internal geometries critical to favorable regeneration outcomes – interconnected, spherical macropores and nanofibrous surface texture.



Our ongoing work aims to understand the in vivo implications and feasibility of these materials at a clinical scale for routine dental applications. We are eager to share this work with the field.

**Project completion date:** 8/31/23

**Journal of Oral Implantology Manuscript Submission Date:** Manuscript in preparation

**Project expenses:** See attached financial report.